

Spatial variation of overbank aggradation rate and its influence on avulsion frequency

TORBJÖRN E. TÖRNQVIST* and JOHN S. BRIDGE†

**Department of Earth and Environmental Sciences, University of Illinois at Chicago, 845 West Taylor Street, Chicago, IL 60607-7059, USA (E-mail: tor@uic.edu)*

†*Department of Geological Sciences, Binghamton University, PO Box 6000, Binghamton, NY 13902-6000, USA*

ABSTRACT

River avulsions are commonly considered to be driven by the aggradation and growth of alluvial ridges, and the associated increase in cross-valley slope relative to either the down-channel slope or the down-valley slope (the latter is termed the slope ratio in the present paper). Therefore, spatial patterns of overbank aggradation rate over stratigraphically relevant time scales are critical in avulsion-dominated models of alluvial architecture. Detailed evidence on centennial- to millennial-scale floodplain deposition has, to date, been largely unavailable. New data on such long-term overbank aggradation rates from the Rhine–Meuse and Mississippi deltas demonstrate that the rate of decrease of overbank deposition away from the channel belt is much larger than has been supposed hitherto, and can be similar to observations for single overbank floods. This leads to more rapid growth of alluvial ridges and more rapid increase in slope ratios, potentially resulting in increased avulsion frequencies. A revised input parameter for overbank aggradation rate was used in a three-dimensional model of alluvial architecture to study its effect on avulsion frequency. Realistic patterns of avulsion and interavulsion periods (≈ 1000 years) were simulated with input data from the Holocene Rhine River, with avulsions occurring when the slope ratio is in the range 3–5. However, caution should be practised with respect to uncritical use of these numbers in different settings. Evidence from the two study areas suggests that the avulsion threshold cannot be represented by one single value, irrespective of whether critical slope ratios are used, as in the present study, or superelevation as has been proposed by other investigators.

Keywords Alluvial architecture, avulsion, Mississippi delta, overbank deposition, Rhine–Meuse delta.

INTRODUCTION

Avulsion is the relatively sudden shift of a river or distributary channel to a new course on a floodplain or deltaic plain. As a channel belt aggrades and forms an alluvial ridge, the increase over time in the ratio of its cross-valley to down-channel slope can be a dominant mechanism driving avulsions (e.g. Allen, 1965; Wells & Dorr, 1987; Brizga & Finlayson, 1990; Slingerland & Smith, 1998; Jones & Schumm, 1999). Others have invoked the elevation of the alluvial ridge above the adjacent flood basin (superelevation) as a

parameter controlling avulsion (Bryant *et al.*, 1995; Heller & Paola, 1996; Mohrig *et al.*, 2000). The exact timing and location of avulsions is also related to temporally or spatially intermittent phenomena (reviewed by Jones & Schumm, 1999) such as extreme peak discharges, ice jams, beaver dams and channels that link the channel belt to the flood basin (e.g. crevasse channels or residual channels of older channel belts).

Spatial variability in overbank aggradation rate is the main control on the slope ratio, defined in this paper (following Mackey & Bridge, 1995) as the ratio between cross-valley slope at the margin

of the channel belt and the down-valley slope of the channel belt. Numerous studies of short-term (single flood) to medium-term (decadal to centennial scale) floodplain aggradation demonstrate a decrease in deposition rate, thickness and mean grain size of overbank deposits away from the active channel (e.g. Marriott, 1992; Guccione, 1993; Walling *et al.*, 1996; Middelkoop & Asselman, 1998). However, the relationship between deposition rate during single major floods and rates over longer time scales more relevant for the stratigraphic record remains uncertain (Bridge & Leeder, 1979; Bridge & Mackey, 1993). Real-world data providing detailed spatial patterns of long-term (centennial to millennial scale) overbank aggradation rates are currently virtually non-existent. This is particularly true for wide floodplains, where hydraulics and sedimentation are controlled by the depositional system itself and are not constrained by a limited valley width.

There is a pressing need for more dedicated field data to calibrate, validate and improve process-based models of floodplain aggradation and alluvial architecture (e.g. Howard, 1992, 1996; Mackey & Bridge, 1995; Heller & Paola, 1996; Paola, 2000). At present, quantitative field data deliberately aimed at testing such models (e.g. Leeder *et al.*, 1996) are limited, partly reflecting the relatively slow pace at which these data accumulate compared with model development (Blum & Törnqvist, 2000; Paola, 2000).

The objectives of this paper are (1) to present new data on spatially variable, long-term (centennial to millennial scale) overbank aggradation rates; (2) to use this evidence to explore the sensitivity of avulsion frequency to different geometries of overbank aggradation; and (3) to compare the analysis of the occurrence of avulsion using slope ratios with alternative approaches that focus on superelevation. This study uses the process-based three-dimensional alluvial architecture model of Mackey & Bridge (1995), which simulates the spatial distribution of channel-belt deposits in alluvial strata as a function of a range of variables, including overbank aggradation rate and avulsion frequency (Fig. 1). This model has previously been shown to agree qualitatively with (1) the different modes of avulsion in modern rivers, such as the Yellow River (e.g. Li & Finlayson, 1993), the Po River (e.g. Nelson, 1970) and the Kosi River (e.g. Wells & Dorr, 1987); (2) the association of high avulsion frequency with high deposition rates and high slope ratios, as reconstructed from Holocene environments by Törnqvist (1994), observed experimentally for steep alluvial fans by Bryant

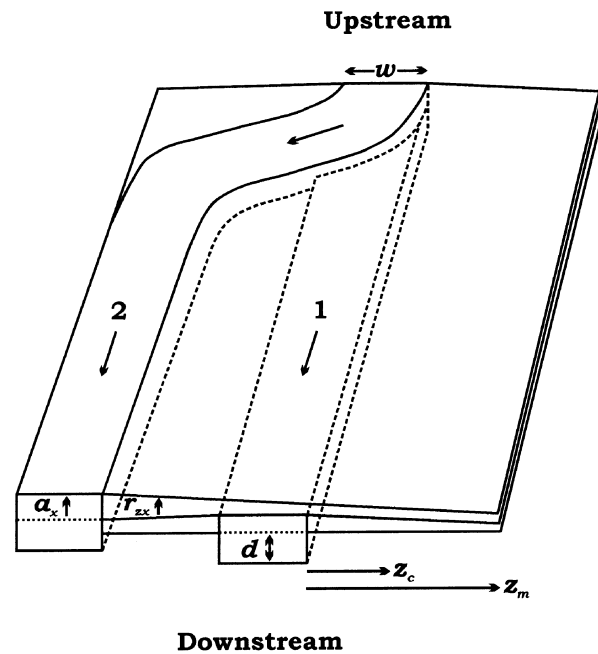


Fig. 1. Floodplain definition diagram with rectangular channel belts with width w and incised bankfull channel depth d . The channel belts aggraded at rate a_x , and adjacent floodplain surfaces at rate r_{zx} , which decreases with increasing distance z_c from the channel-belt edge. z_m is the notational maximum cross-valley extent of overbank deposition. The overall thickness of channel belt (1) equals the aggraded thickness plus the bankfull channel depth. Channel-belt and overbank deposits are compacted just before an avulsion. A new channel belt (2) is then incised on the floodplain surface, and the process of aggradation and compaction is repeated until the next avulsion occurs.

et al. (1995) and predicted theoretically by Slingerland & Smith (1998); and (3) the effect of tectonic tilting on the mode of avulsion and the spatial distribution of channel belts (e.g. Alexander *et al.*, 1994; Leeder *et al.*, 1996; Peakall, 1998; Peakall *et al.*, 2000). This model also quantitatively simulated the observed modes of avulsion and general distribution of channel-belt deposits of the Holocene Lower Mississippi valley and Mississippi delta (Bridge, 1999).

MODEL COMPONENTS

Overbank aggradation rate

Several workers have proposed quantitative models for overbank deposition (e.g. Bridge & Leeder, 1979; James, 1985; Pizzuto, 1987; Howard, 1992, 1996; Bridge & Mackey, 1993; Marriott, 1996; Juergens Gross & Small, 1998; Hardy *et al.*, 2000), but this process is represented mathematically

with different degrees of sophistication. In the three-dimensional model of Mackey & Bridge (1995), overbank aggradation rate, r_{zx} , averaged over the time period separating avulsions, is described by the empirical expression

$$r_{zx} = a_x e^{-bz_c/z_m} \quad (1)$$

where a_x is the channel-belt aggradation rate at down-valley distance x , z_c is the cross-valley distance from the channel-belt edge, z_m is a notional maximum distance of overbank deposition from the channel-belt edge (discussed in more detail below), and b is the overbank aggradation exponent. Exponent b defines the rate of decrease of the time-averaged overbank aggradation rate with distance from the channel belt (Fig. 2).

Values of b (0.35–1.4) estimated by Bridge & Mackey (1993) are based on data published by Pizzuto (1987), representing floodplain deposition by one small stream during the last few centuries. As stated by Bridge & Leeder (1979) and Bridge & Mackey (1993), single-flood data may not be representative of overbank aggradation over longer time scales. Indeed, the b exponent for single-flood (short-term) overbank deposits is usually an order of magnitude higher, with values of 5–10 (Bridge & Mackey, 1993; based on data from Kesel *et al.*, 1974) or ≈ 5 (Middelkoop & Asselman, 1998). This would suggest that b decreases as the time span of observation increases. An alternative approach (Goodbred & Kuehl, 1998; Walling, 1999 and references therein) uses ^{137}Cs and ^{210}Pb radionuclides to study floodplain aggradation over medium-term time scales up to ≈ 100 years. However, in most cases, much longer time spans of measurement are required to assess the relation-

ship between overbank aggradation, avulsion and the stratigraphic record.

Several recently proposed floodplain deposition models (e.g. Howard, 1992, 1996; Nicholas & Walling, 1997; Middelkoop & Van der Perk, 1998; Hardy *et al.*, 2000) have incorporated the influence of floodplain topography on short-term overbank aggradation rate. For the geologic time scales that are of more relevance in the context of alluvial architecture, it is assumed that floodplain relief will be smoothed out and will be of less overall importance. Nevertheless, as will be discussed below, complex floodplain topography may influence overbank deposition under some circumstances.

Avulsion

The probability of an avulsion [$P(a)$; $P(a) \leq 1$] is defined in the Mackey & Bridge (1995) model by

$$P(a) = \left(\frac{Q_f}{Q_a}\right)^{e_Q} \left(k_s \frac{S_{cv}}{S_{dv}}\right)^{e_S} \quad (2)$$

where Q_f is the maximum flood discharge for a given year, Q_a is the threshold discharge necessary for an avulsion given an appropriate slope ratio, S_{cv} is the local cross-valley slope at the edge of the channel belt, S_{dv} is the local down-valley slope of the channel belt, k_s is the avulsion slope constant, and e_Q and e_S are the avulsion discharge exponent and avulsion slope exponent respectively. Avulsion probabilities are calculated at each time step in the model for each cross-valley transect and then compared with a random number from a uniform distribution ranging from 0 to 1. If any local $P(a)$ exceeds the random

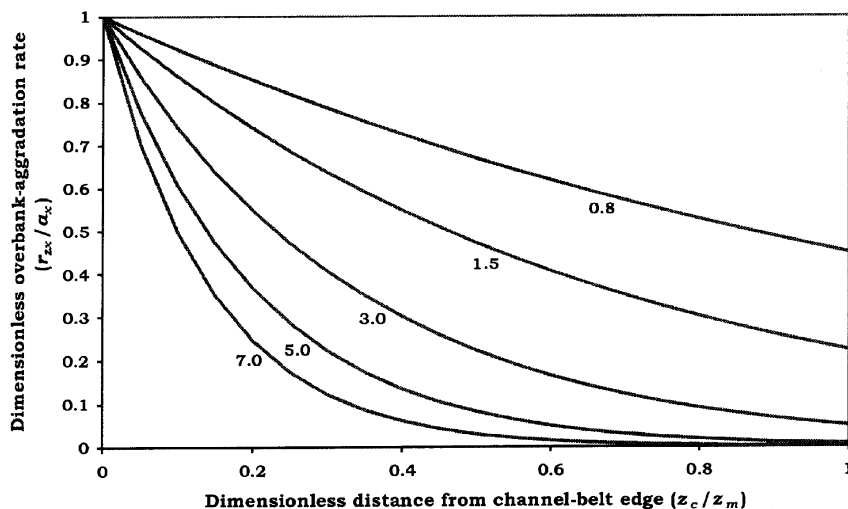


Fig. 2. Series of curves illustrating the decrease in overbank aggradation rate as a function of the distance from the channel-belt edge for labelled values of the overbank aggradation exponent b .

number, an avulsion is initiated. If there is more than one possible avulsion location, the point with the highest value for $P(a)$ is selected. The likelihood of an avulsion increases as the terms on the right-hand side of Eq. (2) approach unity. The avulsion slope constant was introduced to control the slope ratio at which an avulsion becomes a certainty given a sufficiently high-magnitude flood. For example, if k_s is 0.2, the slope ratio term is unity if the slope ratio is 5 (i.e. the avulsion slope constant is the inverse of the critical slope ratio). The exponents were introduced to limit the avulsion probability. For example, if the exponents are large positive numbers, the avulsion probability is only close to unity if the discharge ratio and the slope ratio terms are close to unity.

A key characteristic of the three-dimensional model of Mackey & Bridge (1995), compared with its two-dimensional predecessors (Bridge & Leeder, 1979; Bridge & Mackey, 1993), is that avulsion location and frequency can be simulated as dependent parameters. Equation (2) predicts that the probability of avulsion increases as an alluvial ridge grows, that is as the slope ratio increases. As spatial variation in overbank aggradation rate is an important control of the slope ratio, it is a key factor in determining the location and frequency of avulsions. Model output can be compared with evidence on interavulsion periods (i.e. periods of activity of individual channel belts; *sensu* Törnqvist, 1994) over Holocene time scales, such as those available from the Rhine–Meuse delta (Törnqvist, 1994; Berendsen & Stouthamer, 2001; Stouthamer & Berendsen, 2001), the Mississippi delta (Törnqvist *et al.*, 1996) and the Saskatchewan River (Morozova & Smith, 1999, 2000).

STUDY AREAS

Holocene overbank deposits in the Rhine–Meuse delta (The Netherlands) and the Mississippi delta (Louisiana, USA) were selected according to the following criteria: (1) they can be attributed unequivocally to one distinct distributary channel belt, i.e. the overbank deposits occur at the surface and are underlain by a distinct peat bed separating them from underlying clastic deposits; (2) they can be distinguished from overbank deposits belonging to laterally adjacent channel belts at the same stratigraphic level, i.e. the distance to such channel belts is of the order of tens of kilometres; (3) they represent the full period of activity of the

channel belt; and (4) there is a sufficient number of boreholes penetrating the overbank sediments. Both study areas are located in the upper deltaic plain where overbank deposition occurred in a strictly freshwater environment, upstream of the realm of delta-lobe progradation.

The $\approx 10 \text{ km}^2$ study area in the Rhine–Meuse delta is located near the Linge, a meandering river with well-developed point bars (Törnqvist, 1993a; Berendsen & Stouthamer, 2001), and contains 434 boreholes (Figs 3 and 4). The relatively straight Bayou Lafourche is a trunk distributary in the Mississippi delta (Fig. 5), which, in contrast to the Linge, has been laterally stable, resulting in a much lower channel-belt width/thickness ratio (Fisk, 1952). Overbank deposits of Bayou Lafourche were analysed in one line of section perpendicular to the channel belt, representative of a $\approx 30 \text{ km}^2$ study area with ≈ 100 boreholes.

In both study areas, at least 95% of the boreholes penetrate the entire overbank succession into the underlying peat. Borehole depths are typically 2–4 m in the Linge area, and 4–16 m in the Bayou Lafourche area. Recognition of overbank deposits as opposed to channel-belt deposits is straightforward in both study areas. Overbank facies are predominantly muddy (clayey or silty; Figs 4 and 5), whereas channel-belt deposits consist primarily of sand (Fig. 5) and, in the case of the Linge in particular, have a distinct morphological expression including residual channels. In addition, the channel belts have eroded the wood peat that underlies the overbank deposits. Hence, the presence or absence of this peat bed is an important criterion in determining the boundary of the channel belt (numerous examples from the Rhine–Meuse delta are provided by Berendsen, 1982; Törnqvist, 1993b; Makaske, 1998; Berendsen & Stouthamer, 2001). In both study areas, the boundary of the channel belt could be determined to within 200 m.

The beginning of activity of the two fluvial systems was dated by AMS (accelerator mass spectrometry) ^{14}C measurement of terrestrial macrofossils extracted from the top of the peat underlying the overbank deposits. There is no evidence for periods of non-deposition at the transition from organic to clastic deposits. The Linge came into existence $\approx 200 \text{ BC}$ and was closed off due to upstream damming of the channel around AD 1300 (Törnqvist & Van Dijk, 1993). It is generally assumed that the Linge was already largely abandoned before this date. Bayou Lafourche originated at AD 450 (Törnqvist *et al.*, 1996) and was dammed early in the twentieth

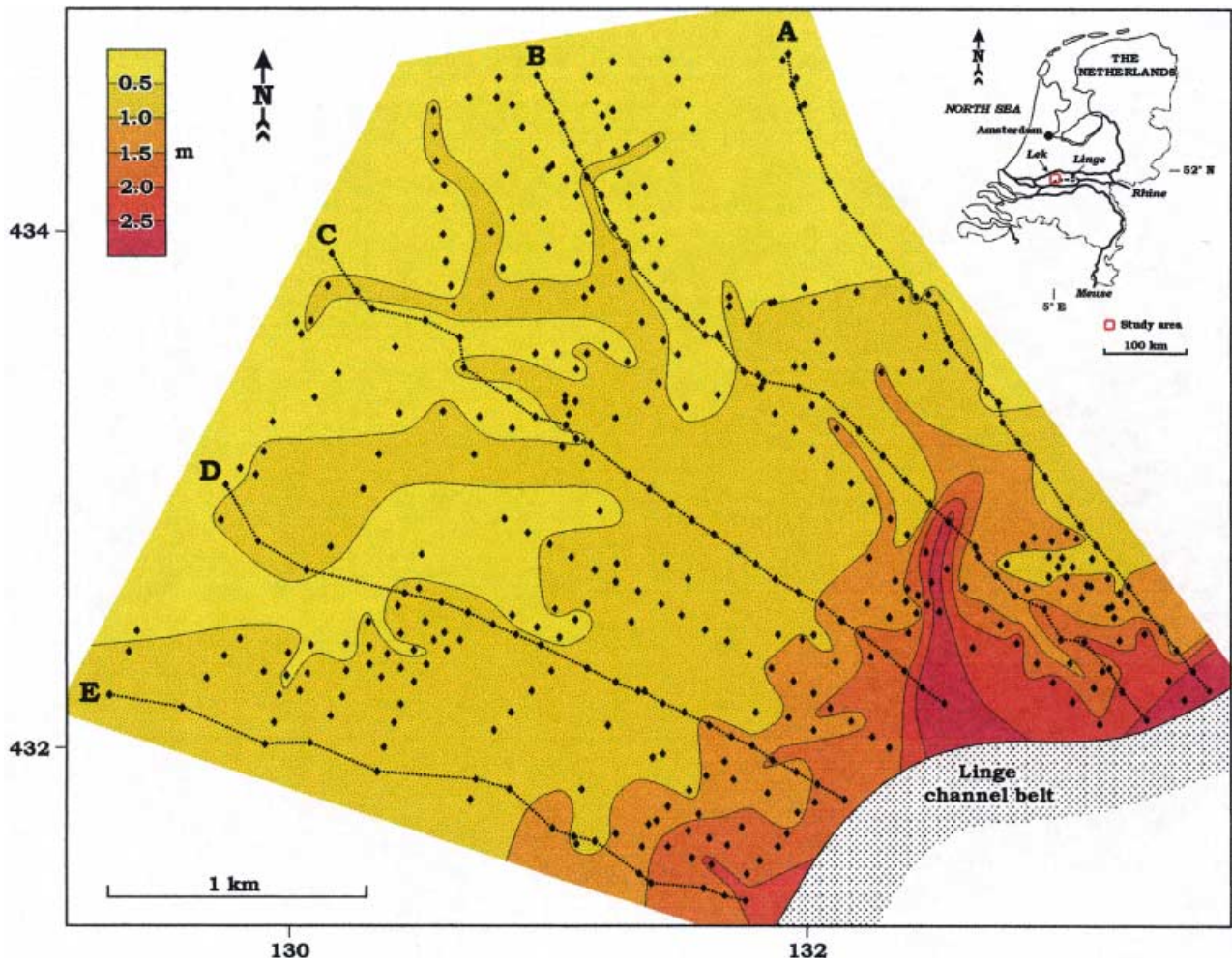


Fig. 3. Map of the Linge area with borehole locations, contours indicating thickness of overbank deposits and lines of section that were subjected to regression analysis. Local (Dutch) co-ordinates indicate the exact location of the study area.

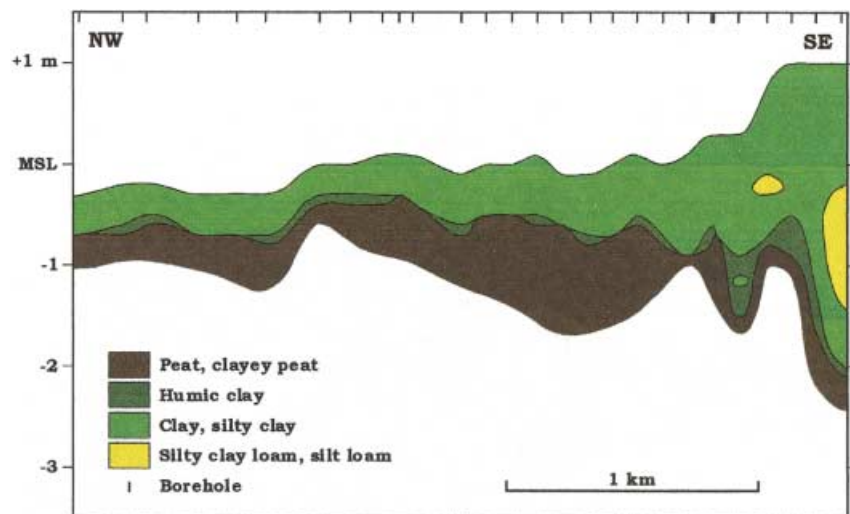


Fig. 4. Cross-section with overbank deposits of the Linge (line of section C; for location, see Fig. 3). The edge of the channel belt is located <50 m south-east of the line of section. MSL, mean sea level.

Fig. 5. Cross-section with overbank deposits of Bayou Lafourche (after Tornqvist et al., 1996). The residual channel of Bayou Lafourche is located 50 m north-east of the line of section. UTM co-ordinates indicate the exact location of the cross-section. MSL, mean sea level.

century but, by then, its discharge had decreased considerably. Hence, these two cases provide evidence on spatially variable overbank aggradation rates over a time interval of 1500 years, an order of magnitude longer and with a much higher level of detail than any currently available data set.

ANALYSIS OF OVERBANK AGGRADATION RATES

Figures 3 and 4 show a rather abrupt decrease in the thickness of overbank deposits proximal to the Linge channel belt and nearly constant values in more distal locations. Five lines of section,

each oriented normal to the channel belt (locations shown in Fig. 3), were used to carry out least-squares regression analyses with the Mackey & Bridge (1995) equation (Eq. 1). This analysis requires an estimate of distance from the edge of the channel belt to the notional edge of the floodplain, z_m . The overbank aggradation rate at $z_c - z_m$ is equal to $a_x e^{-b}$. Therefore, when fitting this equation to field data, it is necessary to define the edge of the channel belt and the notional edge of the floodplain where floodplain deposition rate equals $a_x e^{-b}$. As the Linge is located in the central part of the Rhine-Meuse delta, it is fair to assume that overbank deposition by this distributary terminated well within the limits of the deltaic plain. A value for z_m of 5 km was chosen based on

the fact that the Linge overbank deposits merge with those of another distributary system (the Lek; Törnqvist, 1993b), located about 12 km to the north (Fig. 3).

A characteristic example of a regression analysis applied to the Linge deposits is provided in Fig. 6. As can be seen in Fig. 3, the thickness of proximal Linge overbank deposits is spatially variable, with values ranging from 1.6 to 3.1 m. The curve-fitting results for the five lines of section (Table 1) reflect this variation, with b exponents ranging from 3 to 7. Although correlation coefficients are consistently high (0.87–0.93), the regression line in Fig. 6 shows that, at distances >2 km from the channel-belt edge, overbank deposit thicknesses may be underestimated.

An identical regression analysis was carried out for the Bayou Lafourche data set (Fig. 5), using a value for z_m of 15 km. This is based on cross-

sections from Frazier (1967) showing that overbank deposits of Bayou Lafourche merge laterally with those of Bayou Teche (Fig. 5), located ≈ 40 km to the west. There is excellent agreement between data points and the fitted curve (Fig. 7). These data also show that, in a distributary system formed by a distinctly different fluvial style from the Linge (straight and laterally stable vs. meandering), the b exponent is remarkably similar (Table 1).

As indicated above, the definition of z_m is arbitrary. In both examples, the overbank deposits can be assumed to terminate well within the limits of the deltaic plain, but they are known to merge laterally with overbank sediments from other channel belts, making it difficult to determine their exact limit. In the case of Bayou Lafourche, assuming values for z_m ranging from 5 to 30 km (Fig. 8) results in b -values in the range 2–12. Although this adds considerable

Fig. 6. Characteristic example of regression analysis of overbank deposit thickness vs. distance perpendicular to the Linge channel belt (line of section A; for location, see Fig. 3). As the overbank aggradation interval (≈ 1500 years) is equal throughout the study area, overbank deposit thickness is proportional to overbank aggradation rate.

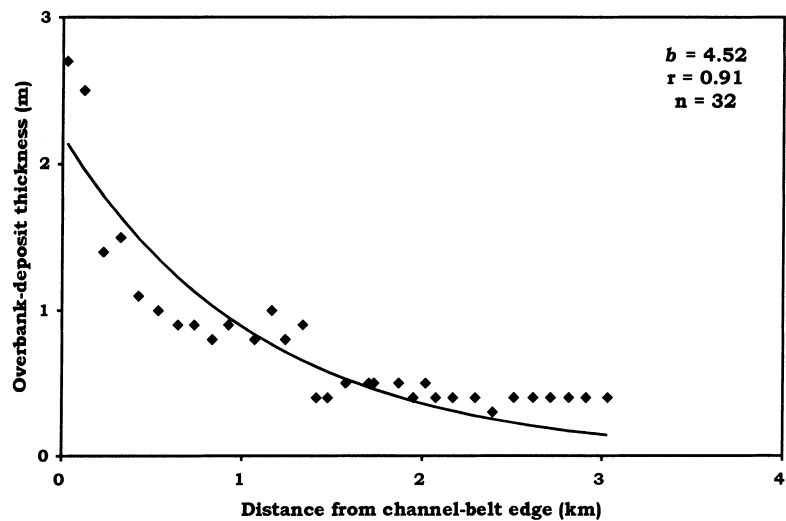


Table 1. Results of regression analyses of overbank deposit thickness for cross-sections perpendicular to the channel belt in the Linge and Bayou Lafourche study areas.

	Cross-section					
	Linge A	Linge B	Linge C	Linge D	Linge E	Bayou Lafourche
Channel-belt aggradation (m)*	2.19	2.42	3.57	1.52	1.97	11.19
Overbank aggradation exponent b^\dagger	4.52	3.21	6.65	3.05	3.39	5.89
Correlation coefficient	0.91	0.88	0.93	0.91	0.87	0.99
Number of data points	32	39	28	22	15	33

* Channel-belt aggradation is proportional to channel-belt aggradation rate (a_x) because the period of activity is ≈ 1500 years in each case; in reality, this value represents proximal overbank aggradation that is greater than channel-belt aggradation because of high compaction rates of strata underlying proximal overbank deposits.

† Calculation of b based on $z_m = 5$ km for Linge and $z_m = 15$ km for Bayou Lafourche.

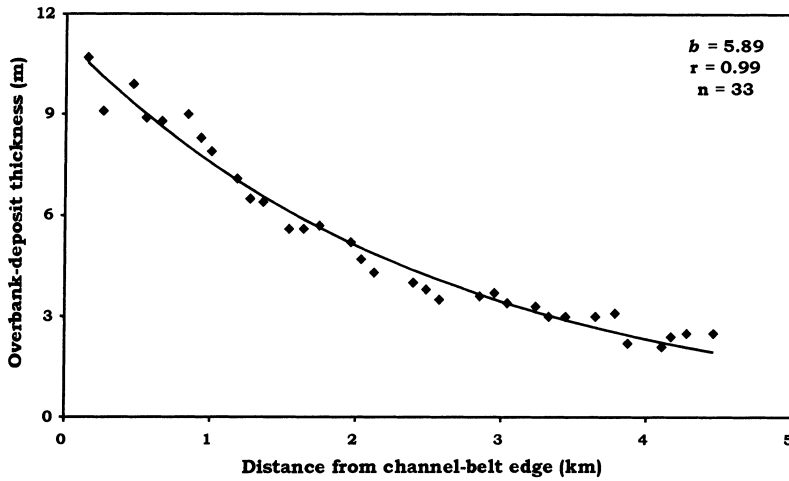


Fig. 7. Regression analysis of overbank deposit thickness vs. distance perpendicular to the Bayou Lafourche channel belt, based on the cross-section in Fig. 5.

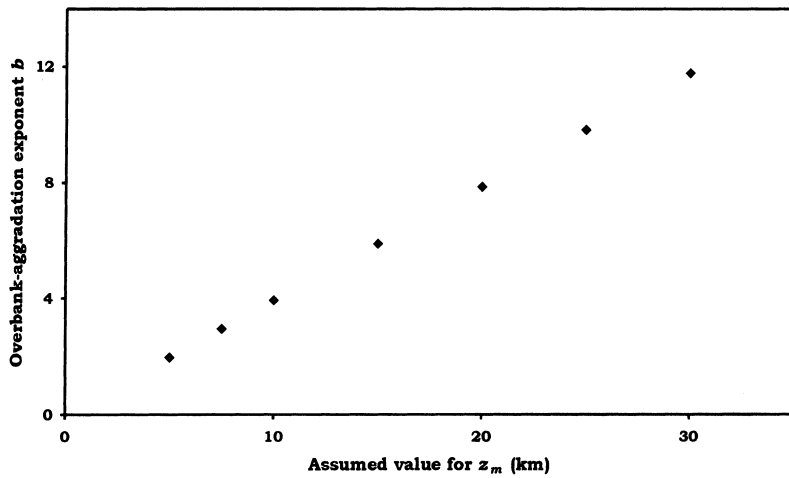


Fig. 8. The effect of variable z_m on the calculated b exponent for the Bayou Lafourche data.

uncertainty to the calculations, it does not change the conclusion that the decrease in the rate of overbank aggradation away from the channel belt is almost an order of magnitude greater than has been assumed based on previously available data.

MODEL EXPERIMENT

Mackey & Bridge (1995) presented a large number of experiments with their model, assessing the role of a wide variety of input parameters. However, the b exponent was held constant at 0.8. In a more recent paper (Bridge, 1999), a value of 0.3 was used for a simulation of the Mississippi delta. For the present study, a sensitivity experiment was performed (cf. Oreskes *et al.*, 1994) using alternative b exponents, guided by the field evidence discussed above. The goal was to simu-

late a Holocene succession as produced by a typical Rhine distributary based on five successive avulsions.

Input parameters for model runs are listed in Table 2. Because the specific focus is on the relationship between overbank deposition rate and avulsion frequency, the role of discharge in the avulsion component of the model (Eq. 2) has been removed by setting the avulsion discharge exponent (e_Q) to zero. This means that the discharge term in Eq. (2) is unity, and that avulsions will occur more frequently than if this term was variable and less than unity, as it would be normally. This also means that, once the slope ratio term reaches unity as the alluvial ridge grows in relief, the probability of avulsion will be unity (i.e. a certainty). As tectonism was not incorporated in the experiments, all stochastic components were removed, enabling a deterministic analysis based on a limited number of model runs.

Table 2. Input parameters of the three-dimensional alluvial architecture model for Rhine simulation.

Up-valley floodplain width	5 km
Down-valley floodplain width	7 km
Floodplain length	20 km
Initial floodplain slope	0.00025
Down-valley slope exponent	0
Channel-belt width	500 m
Maximum bankfull channel depth	7 m
Channel-belt aggradation rate	1 mm year ⁻¹
Down-valley aggradation exponent	-0.2
Avulsion discharge exponent	0
Avulsion slope exponent	10
Aggradation interval (time step)	10 years
Overbank aggradation exponent b	0.8, 1.5, 3.0, 5.0, 7.0
Avulsion slope constant k_s	0.2, 0.3, 0.5

Values for the b exponent of 0.8, 1.5, 3.0, 5.0 and 7.0 were used, approximately covering the range from previously used values to the highest values derived from our regression analyses. The avulsion slope constant (k_s) was used as a calibration parameter and ranged from 0.2 to 0.5. This means that, if the slope ratio at the channel-belt edge exceeds 2 (for $k_s = 0.5$) or 5 (for $k_s = 0.2$), avulsion becomes a certainty. The goal was to obtain model runs with realistic interavulsion periods for each of the five channel belts, compared with measured interavulsion periods from the Rhine–Meuse delta. Typical interavulsion periods for Rhine distributaries are 1180 ± 490 calendar years (Törnqvist, 1994) or 1280 ± 820 calendar years (Stouthamer & Berendsen, 2001).

Table 3. Interavulsion periods for 15 model runs simulating five successive Rhine avulsions.

Overbank aggradation exponent (b)	Avulsion slope constant (k_s)	IAP-1*	IAP-2	IAP-3	IAP-4	IAP-5
0.8	0.2	5020	4000	10	10	10
0.8	0.3	3730	3310	10	130	10
0.8	0.5	2390	1810	470	910	400
1.5	0.2	3110	3060	270	10	10
1.5	0.3	2170	1990	660	10	10
1.5	0.5	1350	1180	220	10	10
3.0	0.2	1680	1640	450	160	10
3.0	0.3	1150	1160	190	10	10
3.0	0.5	710	450	280	10	10
5.0	0.2	1060	870	190	10	10
5.0	0.3	720	550	10	10	10
5.0	0.5	440	220	360	10	10
7.0	0.2	780	730	10	10	10
7.0	0.3	530	470	10	10	10
7.0	0.5	320	240	30	10	10

* IAP, interavulsion period (years).

The outcomes of 15 model runs are summarized in Table 3. As expected, avulsion frequency increases as b and k_s increase. As b increases, slope ratios increase more rapidly, which inevitably leads to higher avulsion frequencies (i.e. lower interavulsion periods). The avulsion frequency also increases with successive avulsions because the alluvial ridge is progressively increasing in relief, ultimately leading to the attainment of critical slope ratios (i.e. avulsion is a certainty) everywhere along the channel-belt edge. Once this is the case (typically after two to five avulsions), an avulsion occurs at every time step (10 years) because the discharge ratio (Eq. 2) was artificially set to unity. Therefore, the field data must only be compared with the model results before this critical condition.

Realistic modes and frequencies of avulsion occur when $b = 0.8$ and $k_s = 0.5$, $b = 3.0$ and $k_s = 0.2$ – 0.3 or $b = 5.0$ and $k_s = 0.2$ (Table 3). Figure 9 shows an example of a realistic model result. These results imply that the effect of increasing avulsion frequency with an increased b exponent can be countered by reducing the avulsion slope constant.

DISCUSSION

Overbank aggradation rate

The regression analyses demonstrate that values for the overbank aggradation exponent, b , for time scales of hundreds to thousands of years are similar to those for single floods (typical values

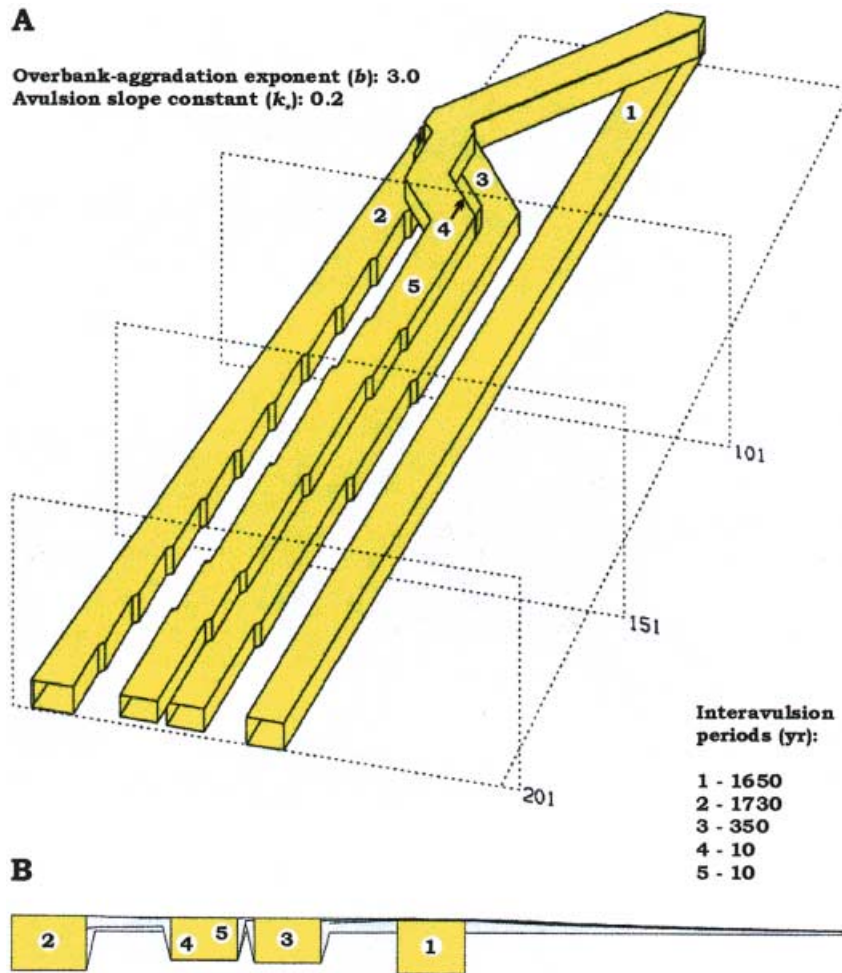


Fig. 9. Example model run of five successive Rhine avulsions with $b = 3.0$ and $k_s = 0.2$, illustrated by (A) a three-dimensional panel and (B) a strike-oriented cross-section at the downstream end of the floodplain. Note that the outcomes of this run are slightly different from the equivalent run in Table 3 because of a different sequence of random numbers.

of ≈ 5), and not substantially less (0.35–1.4) as suggested by Bridge & Mackey (1993). Increased b -values imply decreased overbank aggradation rates in areas away from the active channel belt and more rapidly increasing cross-valley slopes of the developing alluvial ridge. The data reported by Pizzuto (1987) have previously played an important role in assumptions for the b exponent by Bridge & Mackey (1993). It should be noted that the field area detailed by Pizzuto (1987) constituted a narrow floodplain in a bedrock valley with very limited vertical aggradation, a setting that may be less than ideal in the context of modelling alluvial architecture.

Studies of contemporary floodplain aggradation show that sand deposition commonly decreases abruptly away from the channel, whereas mud usually accumulates as a more continuous blanket (e.g. Marriott, 1992; Guccione, 1993; Asselman & Middelkoop, 1995; Walling *et al.*, 1996; Middelkoop & Asselman, 1998). The new data, particularly those from the Linge, demonstrate an

abruptly decreasing thickness of proximal overbank deposits, giving way to a homogeneous clay bed with a fairly constant thickness of ≈ 0.4 m in more distal settings. This is consistent with numerous previous reports based on Holocene data from the Rhine–Meuse delta (e.g. Berendsen, 1982; Van der Woude, 1983; Törnqvist, 1993b, 1994), although exceptions also occur (see below). These observations call for a slightly revised approach to simulating overbank aggradation rate in alluvial architecture models. Several studies have incorporated a location-independent, floodplain-wide minimum aggradation rate (Howard, 1992, 1996; Walling *et al.*, 1996; Karssen *et al.*, 2001). The new data suggest that such a representation may be more realistic, although the situation is further complicated on wide floodplains or deltaic plains where overbank deposition does not always extend to the edge of the basin. Therefore, a potentially more successful approach might be to define z_m as the distance at which an abrupt decrease in

overbank aggradation rate gives way to more constant values. If $z_c > z_m$, the overbank deposition rate is still finite and continues to decrease with increasing z_c , but the rate of decrease in overbank deposition rate is small. Such an approach has the potential of providing a better fit of regression lines to the data points.

The exponential expression for overbank aggradation rate results in wedge-shaped deposits with smooth boundaries over the time interval between avulsions. However, numerous floodplains are dominated by spatially complex crevasse splays or lacustrine deltas, with much more variable topography (e.g. Smith *et al.*, 1989; Tye & Coleman, 1989; Törnqvist, 1993a; Weerts & Bierkens, 1993; Smith & Pérez-Arlucea, 1994). Such settings may require a stochastic component in the modelling of overbank deposition (cf. Bridge & Leeder, 1979), for instance based on geostatistical parameters (Weerts & Bierkens, 1993).

It must finally be stressed that the high b exponents in the present cases do not apply directly to the topographic slope at the surface. The relationship between b and S_{cv} may be less than straightforward if differential compaction has occurred. Compaction of organic beds underlying overbank deposits is an important process in both study areas. As wood peat forms close to the water table, the land surface must have been essentially horizontal immediately before overbank deposition. In neither of the cross-sections (Figs 4 and 5) is there evidence for erosion of the wood peat. On the contrary, multiple, isochronous ^{14}C ages from the top of this peat bed have been reported from both study areas (Törnqvist & Van Dijk, 1993; Törnqvist *et al.*, 1996). The rapid decrease in the thickness of overbank deposits has caused substantial differential compaction of at least 1.5 m (Linge area) or 5 m (Bayou Lafourche area), as can be determined from the deformation of the top of the peat bed in the two cross-sections. In these examples, compaction accommodates roughly half the thickness of proximal overbank deposits. Similar observations have been made by Nadon (1998), who demonstrated the important role of compaction of peats at shallow depths. In contrast, compaction of mud in floodplain locations distant from the channel belt may have the opposite effect of increasing cross-valley slopes, but this effect is likely to be less prevalent. Therefore, it can be concluded that (1) the b exponent, as far as being related to the cross-valley slope, will in reality be somewhat lower than calculated using Eq. (1) for cases with abundant organics in the subsurface; and (2) it is

desirable that future generations of alluvial architecture models compute compaction at every time step, and not only immediately before an avulsion, as in Mackey & Bridge (1995).

Avulsion

In the experiments presented here, avulsions have a high probability of occurring when the slope ratio is between about 3 and 5. In the terminology of Jones & Schumm (1999), this critical slope ratio constitutes the 'avulsion threshold'. Guccione *et al.* (1999) calculated a slope ratio of 4.2 that caused a partial avulsion in the Lower Mississippi valley. However, they used the ratio between cross-valley slope and down-channel slope of the Mississippi River, and not of the channel belt, as used in the model of Mackey & Bridge (1995). Peakall *et al.* (2000) report slope ratios of 1–5 for avulsing rivers influenced by tectonic tilting, although their cross-valley slopes have been calculated for longer distances away from the channel belts than in the Rhine simulations. Theoretical predictions by Slingerland & Smith (1998), which consider how hydraulics and suspended sediment load control enlargement or filling of a crevasse channel, suggest that avulsions are most likely when the ratio between the bed slope of the crevasse channel and main channel exceeds ≈ 5 . Despite the similarity to the results from the present study, it remains to be established whether this relationship will hold once such theories also consider the all-important bedload.

Mohrig *et al.* (2000) argued that the height of natural levees above the adjacent flood basin divided by channel depth (the normalized super-elevation) for modern, avulsing rivers exhibits less scatter (typical values of ≈ 0.5) than the ratio between cross-valley slope and down-channel slope (which varies by an order of magnitude). These authors investigated Tertiary alluvial-fan deposits, where they measured mean normalized super-elevations of 0.6–1.1. Bayou Lafourche, representative of alluvial ridges in the Mississippi delta, has a natural levee height of 5 m (Fig. 5). As flow depths in the Mississippi delta can be up to 60 m, normalized super-elevation is < 0.1 , an order of magnitude lower than the field data of Mohrig *et al.* (2000), and substantially lower than data from other rivers presented by these authors.

On the other hand, the slope ratio for Bayou Lafourche, measured from the crest of the natural levee (at 6 m above sea level) yields a value of 25

($S_{cv} = 0.001$ for the proximal 4 km of the natural levee; $S_{dv} = 0.00004$ for the 145 km distance to the coast), an order of magnitude higher than critical slope ratios inferred from simulations of the Rhine as discussed in the present paper.

These observations give the impression that both the normalized superelevation and the critical slope ratio for avulsing rivers exhibit considerable scatter. Considering the controversy between the critical slope ratio as determined by the present model and the value estimated for Bayou Lafourche, it is important to note that the initial floodplain slope at the beginning of the model runs was set at 0.00025 (the slope of the Pleistocene basement in the Rhine–Meuse delta), an order of magnitude higher than the slope of Bayou Lafourche. In conclusion, it is suspected that the avulsion threshold, whether represented by the slope ratio or by normalized superelevation, may be substantially different in low-gradient settings (e.g. lower deltaic plains) than in high-gradient settings (e.g. alluvial fans).

An increased overbank aggradation exponent leads to a relatively slow burial of abandoned alluvial ridges, which therefore exert a stronger control on the courses of younger channel belts that are preferentially located in the lowest parts of flood basins. However, reoccupation of residual channels of older channel belts has long been recognized as an important process (e.g. Fisk, 1952; Wells & Dorr, 1987; Smith *et al.*, 1998; Mohrig *et al.*, 2000). Currently available data suggest that avulsion by reoccupation of pre-existing channels occurs primarily under conditions of reduced aggradation rates (Aslan & Blum, 1999; Morozova & Smith, 1999, 2000).

Several studies have reported that avulsions can also take place in the absence of significant aggradation (e.g. Schumm *et al.*, 1996; Gibling *et al.*, 1998; Jones & Harper, 1998; Mack & Leeder, 1998). Makaske (1998; see also the discussion by Makaske, 2001) has proposed a ‘capacity-based avulsion model’ (as opposed to the ‘topography-based avulsion model’ that underpins alluvial architecture models), which assumes that a limited sediment transport capacity may cause channels to become hydraulically inefficient over time, thus providing an alternative mechanism for avulsions.

Clearly, such alternative mechanisms (channel-belt reoccupation and avulsion without significant aggradation) have major implications for alluvial architecture. Channel-belt reoccupation will lead to recycling of existing channel belts and might reduce channel-deposit proportions

(unless aggradation rates are extremely low), whereas avulsion into topographic lows without aggradation constitutes an opposite scenario. It is therefore essential that future studies focus on the controls determining avulsion style, and that refined models address these phenomena.

Finally, it should be remembered that there are other influences on the nature of avulsion, such as extreme flood discharges, temporary dams that cause backwater effects and deposition upstream, as well as channels that link the channel belt to the flood basin. In the model of Mackey & Bridge (1995), the effects on avulsion frequency of extreme flood discharges are taken account of explicitly, but other controls are only accommodated through the random component of the model. Future studies should focus on a more rational treatment of the full spectrum of controls on avulsion.

CONCLUSIONS

1 This study presents the first detailed data sets of spatially variable overbank aggradation rates averaged over up to 1500 years. Evidence from the Rhine–Meuse and Mississippi deltas demonstrates that the decrease in overbank deposit thickness (proportional to the rate of overbank deposition) away from the channel belt is more abrupt than has so far been assumed, and is approximately similar to observations for single-flood deposits. In addition, there is a tendency for a widespread minimum aggradation rate of overbank muds at considerable distances from the genetically associated channel belt. This, along with the ongoing role of compaction as well as stochastic topographic phenomena (such as crevasse splays and lacustrine deltas), should be taken into account in future generations of alluvial architecture models.

2 An increased overbank aggradation exponent (b), which reflects a more rapidly decreasing overbank aggradation rate away from the channel belt, leads to increased avulsion frequency (disregarding the possible effects of other controls such as discharge variations). Unrealistically low interavulsion periods, a direct implication of high avulsion frequencies, can be countered by decreasing the avulsion slope constant (k_s); this implies that higher slope ratios are necessary to initiate avulsions. Simulation of successive avulsions of the Holocene Rhine River suggests that the occurrence of avulsion approaches certainty when the slope ratio enters the range of 3–5

as a result of growth of an alluvial ridge, but caution should be practised against uncritical use of these numbers in different settings. These revisions also lead to much slower burial of abandoned alluvial ridges, which therefore exert more control on the courses of younger channel belts. On the other hand, there is a need for a stronger appreciation of avulsions that may occur without significant aggradation, including the widely observed recycling of channel belts associated with the reoccupation of residual channels.

3 It is unlikely that the threshold for avulsions associated with the growth of alluvial ridges can be defined by one critical value with universal significance. Although this study has focused on the critical slope ratio, other investigations have proposed normalized superelevation as the key parameter driving avulsions. Field evidence from the Rhine–Meuse and Mississippi deltas suggests that neither of the two can be characterized by one single value, but more research into this problem is necessary.

ACKNOWLEDGEMENTS

The main field data (Linge area) were collected by students of physical geography, Utrecht University, in 1990 and 1991. We thank Henk Berendsen for permission to use these data, Nathalie Asselman for insightful discussions about modern floodplain sedimentation, and Rudy Slingerland for comments on an earlier draft. The paper benefited greatly from rigorous and thoughtful reviews by Lawrence S. Jones and Chris Paola.

NOMENCLATURE

α_x	channel-belt aggradation rate at down-valley distance x from point of origin (m year^{-1})
b	overbank aggradation rate exponent
d	maximum bankfull channel depth (m)
e_Q	avulsion discharge exponent
e_S	avulsion slope exponent
k_s	avulsion slope proportionality constant
$P(a)$	probability of an avulsion
Q_a	threshold flood discharge necessary for an avulsion ($\text{m}^3 \text{s}^{-1}$)
Q_f	maximum flood discharge for a given year ($\text{m}^3 \text{s}^{-1}$)

r_{zx}	overbank aggradation rate at distance z_c from channel-belt edge at down-valley distance x from point of origin (m year^{-1})
S_{cv}	local cross-valley slope at the channel-belt edge
S_{dv}	local down-valley channel-belt slope
w	channel-belt width (m)
x	down-valley distance from point of origin, positive in down-valley direction (m)
y	vertical distance from point of origin, positive upwards (m)
z	cross-valley distance from point of origin, zero at floodplain centre (m)
z_c	cross-valley distance away from the channel-belt edge (m)
z_m	notional maximum cross-valley distance of overbank deposition away from the channel-belt edge (m).

REFERENCES

- Alexander, J., Bridge, J.S., Leeder, M.R., Collier, R.E.Ll and Gawthorpe, R.L. (1994) Holocene meander-belt evolution in an active extensional basin, southwestern Montana. *J. Sed. Res.*, **B64**, 542–559.
- Allen, J.R.L. (1965) A review of the origin and characteristics of Recent alluvial sediments. *Sedimentology*, **5**, 89–191.
- Aslan, A. and Blum, M.D. (1999) Contrasting styles of Holocene avulsion, Texas Gulf Coastal Plain, USA. In: *Fluvial Sedimentology VI* (Eds N.D. Smith and J. Rogers), *Int. Assoc. Sedimentol. Spec. Publ.*, **28**, 193–209.
- Asselman, N.E.M. and Middelkoop, H. (1995) Floodplain sedimentation: Quantities, patterns and processes. *Earth Surf. Proc. Land.*, **20**, 481–499.
- Berendsen, H.J.A. (1982) De genese van het landschap in het zuiden van de provincie Utrecht, een fysisch-geografische studie. *Utrechtse Geogr. Stud.*, **25**, 1–255.
- Berendsen, H.J.A. and Stouthamer, E. (2001) *Palaeogeographic Development of the Rhine-Meuse Delta, The Netherlands*. Koninklijke Van Gorcum, Assen, 268 pp.
- Blum, M.D. and Törnqvist, T.E. (2000) Fluvial responses to climate and sea-level change: a review and look forward. *Sedimentology*, **47** (Suppl. 1), 2–48.
- Bridge, J.S. (1999) Alluvial architecture of the Mississippi valley: predictions using a 3D simulation model. In: *Floodplains: Interdisciplinary Approaches* (Eds S.B. Marriott and J. Alexander), *Geol. Soc. London Spec. Publ.*, **163**, 269–278.
- Bridge, J.S. and Leeder, M.R. (1979) A simulation model of alluvial stratigraphy. *Sedimentology*, **26**, 617–644.
- Bridge, J.S. and Mackey, S.D. (1993) A revised alluvial stratigraphy model. In: *Alluvial Sedimentation* (Eds M. Marzo and C. Puigdefábregas), *Int. Assoc. Sedimentol. Spec. Publ.*, **17**, 319–336.
- Brizga, S.O. and Finlayson, B.L. (1990) Channel avulsion and river metamorphosis: the case of the Thomson River, Victoria, Australia. *Earth Surf. Proc. Land.*, **15**, 391–404.
- Bryant, M., Falk, P. and Paola, C. (1995) Experimental study of avulsion frequency and rate of deposition. *Geology*, **23**, 365–368.

- Fisk, H.N.** (1952) *Geological Investigation of the Atchafalaya Basin and the Problem of Mississippi River Diversion*. Waterways Experiment Station, Vicksburg, 145 pp.
- Frazier, D.E.** (1967) Recent deltaic deposits of the Mississippi River: their development and chronology. *Trans. Gulf Coast Assoc. Geol. Soc.*, **17**, 287–311.
- Gibling, M.R., Nanson, G.C. and Maroulis, J.C.** (1998) Anastomosing river sedimentation in the Channel Country of central Australia. *Sedimentology*, **45**, 595–619.
- Goodbred, S.L., Jr and Kuehl, S.A.** (1998) Floodplain processes in the Bengal Basin and the storage of Ganges-Brahmaputra river sediment: an accretion study using ^{137}Cs and ^{210}Pb geochronology. *Sed. Geol.*, **121**, 239–258.
- Guccione, M.J.** (1993) Grain-size distribution of overbank sediment and its use to locate channel positions. In: *Alluvial Sedimentation* (Eds M. Marzo and C. Puigdefábregas), *Int. Assoc. Sedimentol. Spec. Publ.*, **17**, 185–194.
- Guccione, M.J., Burford, M.F. and Kendall, J.D.** (1999) Pemi-scot Bayou, a large distributary of the Mississippi River and a possible failed avulsion. In: *Fluvial Sedimentology VI* (Eds N.D. Smith and J. Rogers), *Int. Assoc. Sedimentol. Spec. Publ.*, **28**, 211–220.
- Hardy, R.J., Bates, P.D. and Anderson, M.G.** (2000) Modelling suspended sediment deposition on a fluvial floodplain using a two-dimensional dynamic finite element model. *J. Hydrol.*, **229**, 202–218.
- Heller, P.L. and Paola, C.** (1996) Downstream changes in alluvial architecture: an exploration of controls on channel-stacking patterns. *J. Sed. Res.*, **66**, 297–306.
- Howard, A.D.** (1992) Modeling channel migration and floodplain sedimentation in meandering streams. In: *Lowland Floodplain Rivers. Geomorphological Perspectives* (Eds P.A. Carling and G.E. Petts), pp. 1–41. John Wiley, Chichester.
- Howard, A.D.** (1996) Modelling channel evolution and floodplain morphology. In: *Floodplain Processes* (Eds M.G. Anderson, D.E. Walling and P.D. Bates), pp. 15–62. John Wiley, Chichester.
- James, C.S.** (1985) Sediment transfer to overbank sections. *J. Hydraul. Res.*, **23**, 435–452.
- Jones, L.S. and Harper, J.T.** (1998) Channel avulsions and related processes, and large-scale sedimentation patterns since 1875, Rio Grande, San Luis Valley, Colorado. *Geol. Soc. Am. Bull.*, **110**, 411–421.
- Jones, L.S. and Schumm, S.A.** (1999) Causes of avulsion: an overview. In: *Fluvial Sedimentology VI* (Eds N.D. Smith and J. Rogers), *Int. Assoc. Sedimentol. Spec. Publ.*, **28**, 171–178.
- Juergens Gross, L. and Small, M.J.** (1998) River and floodplain process simulation for subsurface characterization. *Water Resour. Res.*, **34**, 2365–2376.
- Karssenbergh, D., Törnqvist, T.E. and Bridge, J.S.** (2001) Conditioning a process-based model of sedimentary architecture to well data. *J. Sed. Res.*, **71**, 868–879.
- Kesel, R.H., Dunne, K.C., McDonald, R.C., Allison, K.R. and Spicer, B.E.** (1974) Lateral erosion and overbank deposition on the Mississippi River in Louisiana caused by 1973 flooding. *Geology*, **2**, 461–464.
- Leeder, M.R., Mack, G.H., Peakall, J. and Salyards, S.L.** (1996) First quantitative test of alluvial stratigraphic models: Southern Rio Grande rift, New Mexico. *Geology*, **24**, 87–90.
- Li, S. and Finlayson, B.** (1993) Flood management on the lower Yellow River: hydrological and geomorphological perspectives. In: *Current Research in Fluvial Sedimentology* (Ed. C.R. Fielding), *Sed. Geol.*, **85**, 285–296.
- Mack, G.H. and Leeder, M.R.** (1998) Channel shifting of the Rio Grande, southern Rio Grande rift: implications for alluvial stratigraphic models. *Sed. Geol.*, **117**, 207–219.
- Mackey, S.D. and Bridge, J.S.** (1995) Three-dimensional model of alluvial stratigraphy: theory and application. *J. Sed. Res.*, **B65**, 7–31.
- Makaske, B.** (1998) Anastomosing rivers. Forms, processes and sediments. *Neth. Geogr. Stud.*, **249**, 1–287.
- Makaske, B.** (2001) Anastomosing rivers: a review of their classification, origin and sedimentary products. *Earth-Sci. Rev.*, **53**, 149–196.
- Marriott, S.** (1992) Textural analysis and modelling of a flood deposit: River Severn, U.K. *Earth Surf. Proc. Land.*, **17**, 687–697.
- Marriott, S.B.** (1996) Analysis and modelling of overbank deposits. In: *Floodplain Processes* (Eds M.G. Anderson, D.E. Walling and P.D. Bates), pp. 63–93. John Wiley, Chichester.
- Middelkoop, H. and Asselman, N.E.M.** (1998) Spatial variability of floodplain sedimentation at the event scale in the Rhine-Meuse delta, The Netherlands. *Earth Surf. Proc. Land.*, **23**, 561–573.
- Middelkoop, H. and Van der Perk, M.** (1998) Modelling spatial patterns of overbank sedimentation on embanked floodplains. *Geogr. Ann.*, **80A**, 95–109.
- Mohrig, D., Heller, P.L., Paola, C. and Lyons, W.J.** (2000) Interpreting avulsion process from ancient alluvial sequences: Guadalupe-Matarranya system (northern Spain) and Wasatch Formation (western Colorado). *Geol. Soc. Am. Bull.*, **112**, 1787–1803.
- Morozova, G.S. and Smith, N.D.** (1999) Holocene avulsion history of the lower Saskatchewan fluvial system, Cumberland Marshes, Saskatchewan-Manitoba, Canada. In: *Fluvial Sedimentology VI* (Eds N.D. Smith and J. Rogers), *Int. Assoc. Sedimentol. Spec. Publ.*, **28**, 231–249.
- Morozova, G.S. and Smith, N.D.** (2000) Holocene avulsion styles and sedimentation patterns of the Saskatchewan River, Cumberland Marshes, Canada. *Sed. Geol.*, **130**, 81–105.
- Nadon, G.C.** (1998) Magnitude and timing of peat-to-coal compaction. *Geology*, **26**, 727–730.
- Nelson, B.W.** (1970) Hydrography, sediment dispersal, and recent historical development of the Po River delta, Italy. In: *Deltaic Sedimentation. Modern and Ancient* (Ed. J.P. Morgan), *SEPM Spec. Publ.*, **15**, 152–184.
- Nicholas, A.P. and Walling, D.E.** (1997) Modelling flood hydraulics and overbank deposition on river floodplains. *Earth Surf. Proc. Land.*, **22**, 59–77.
- Oreskes, N., Shrader-Frechette, K. and Belitz, K.** (1994) Verification, validation, and confirmation of numerical models in the earth sciences. *Science*, **263**, 641–646.
- Paola, C.** (2000) Quantitative models of sedimentary basin filling. *Sedimentology*, **47** (Suppl. 1), 121–178.
- Peakall, J.** (1998) Axial river evolution in response to half-graben faulting: Carson River, Nevada, USA. *J. Sed. Res.*, **68**, 788–799.
- Peakall, J., Leeder, M., Best, J. and Ashworth, P.** (2000) River response to lateral ground tilting: a synthesis and some implications for the modelling of alluvial architecture in extensional basins. *Basin Res.*, **12**, 413–424.
- Pizzuto, J.E.** (1987) Sediment diffusion during overbank flows. *Sedimentology*, **34**, 301–317.
- Schumm, S.A., Erskine, W.D. and Tilleard, J.W.** (1996) Morphology, hydrology, and evolution of the anastomosing

- Ovens and King Rivers, Victoria, Australia. *Geol. Soc. Am. Bull.*, **108**, 1212–1224.
- Slingerland, R.** and **Smith, N.D.** (1998) Necessary conditions for a meandering-river avulsion. *Geology*, **26**, 435–438.
- Smith, N.D.** and **Pérez-Arlucea, M.** (1994) Fine-grained splay deposition in the avulsion belt of the lower Saskatchewan River, Canada. *J. Sed. Res.*, **B64**, 159–168.
- Smith, N.D., Cross, T.A., Dufficy, J.P.** and **Clough, S.R.** (1989) Anatomy of an avulsion. *Sedimentology*, **36**, 1–23.
- Smith, N.D., Slingerland, R.L., Pérez-Arlucea, M.** and **Morozova, G.S.** (1998) The 1870s avulsion of the Saskatchewan River. *Can. J. Earth Sci.*, **35**, 453–466.
- Stouthamer, E.** and **Berendsen, H.J.A.** (2001) Avulsion frequency, avulsion duration and interavulsion period of Holocene channel belts in the Rhine-Meuse delta, The Netherlands. *J. Sed. Res.*, **71**, 589–598.
- Törnqvist, T.E.** (1993a) Holocene alternation of meandering and anastomosing fluvial systems in the Rhine-Meuse Delta (central Netherlands) controlled by sea-level rise and sub-soil erodibility. *J. Sed. Petrol.*, **63**, 683–693.
- Törnqvist, T.E.** (1993b) Fluvial sedimentary geology and chronology of the Holocene Rhine-Meuse delta, The Netherlands. *Neth. Geogr. Stud.*, **166**, 1–169.
- Törnqvist, T.E.** (1994) Middle and late Holocene avulsion history of the River Rhine (Rhine-Meuse delta, Netherlands). *Geology*, **22**, 711–714.
- Törnqvist, T.E.** and **Van Dijk, G.J.** (1993) Optimizing sampling strategy for radiocarbon dating of Holocene fluvial systems in a vertically aggrading setting. *Boreas*, **22**, 129–145.
- Törnqvist, T.E., Kidder, T.R., Autin, W.J., Van der Borg, K., De Jong, A.F.M., Klerks, C.J.W., Snijders, E.M.A., Storms, J.E.A., Van Dam, R.L.** and **Wiemann, M.C.** (1996) A revised chronology for Mississippi River subdeltas. *Science*, **273**, 1693–1696.
- Tye, R.S.** and **Coleman, J.M.** (1989) Depositional processes and stratigraphy of fluvially dominated lacustrine deltas: Mississippi delta plain. *J. Sed. Petrol.*, **59**, 973–996.
- Van der Woude, J.D.** (1983) Holocene paleoenvironmental evolution of a perimarine fluvial area. Geology and paleobotany of the area surrounding the archeological excavation at the Hazendonk river dune (Western Netherlands). *Anal. Praehist. Leidensia*, **16**, 1–124.
- Walling, D.E.** (1999) Using fallout radionuclides in investigations of contemporary overbank sedimentation on the floodplains of British rivers. In: *Floodplains: Interdisciplinary Approaches* (Eds S.B. Marriott and J. Alexander), *Geol. Soc. London Spec. Publ.*, **163**, 41–59.
- Walling, D.E., He, Q.** and **Nicholas, A.P.** (1996) Floodplains as suspended sediment sinks. In: *Floodplain Processes* (Eds M.G. Anderson, D.E. Walling and P.D. Bates), pp. 399–440. John Wiley, Chichester.
- Weerts, H.J.T.** and **Bierkens, M.F.P.** (1993) Geostatistical analysis of overbank deposits of anastomosing and meandering fluvial systems; Rhine-Meuse delta, The Netherlands. In: *Current Research in Fluvial Sedimentology* (Ed. C.R. Fielding), *Sed. Geol.*, **85**, 221–232.
- Wells, N.A.** and **Dorr, J.A., Jr** (1987) Shifting of the Kosi River, northern India. *Geology*, **15**, 204–207.

*Manuscript received 24 April 2001;
revision accepted 8 March 2002.*